Chemical Science

ARTICLE

α-D-Gal-cyclophellitol cyclosulfamidate is a Michaelis complex analog that stabilizes therapeutic lysosomal α-galactosidase A in Fabry disease

Received 00th January 20xx,
Accepted 00th January 20xx

DOI: 10.1039/x0xx00000x

Marta Artola[a,b], Christinne Hedberg[a], Rhianna J. Rowland[c], Lluís Raich[d], Kassiani Kytidou[b], Liang Wu[c], Amanda Schaaf[a], Maria Joao Ferraz[b], Gijsbert A. van der Marel[a], Jeroen D. C. Codée[a], Carme Rovira[d,e], Johannes M. F. G. Aerts[b], Gideon J. Davies[c,*], Herman S. Overkleeft[a,*]

Fabry disease is an inherited lysosomal storage disorder that is characterized by a deficiency in lysosomal α-D-galactosidase activity. One current therapeutic strategy involves enzyme replacement therapy, in which patients are treated with recombinant enzyme. Co-treatment with enzyme active-site stabilizers is advocated to increase treatment efficacy; a strategy that requires effective and selective enzyme stabilizers. Here, we describe the design and development of an α-D-*gal*-cyclophellitol cyclosulfamidate as a new class of neutral, conformationally-constrained competitive glycosidase inhibitor that acts by mimicry of the Michaelis complex conformation. We found that D-galactose-configured α-cyclosulfamidate **4** effectively stabilizes recombinant human α-D-galactosidase (agalsidase beta, Fabrazyme®) both *in vitro* and *in cellulo*.

Introduction

Deficiency in α-galactosidase A (α-gal A, EC 3.2.1.22, a retaining glycosidase of the GH27 glycoside hydrolase family (www.cazy.org)[1]) underlies Fabry disease. This inherited lysosomal storage disorder is characterized by toxic accumulation of glycosphingolipid globotriaosylceramide (Gb3) in lysosomes and its sphingoid base, globotriaosylsphingosine (Lyso-Gb3) in plasma and tissues[2,3]. Several mutations in the GLA gene encoding α-gal A can result in diminished protein levels and/or enzyme activity, leading to altered metabolite levels and a range of Fabry disease phenotypes. The accumulation of glycosphingolipid metabolites is thought to cause progressive renal and cardiac insufficiency and CNS pathology in Fabry patients[4]. Enzyme replacement therapy (ERT) for Fabry disease involves intravenous treatment with recombinant human α-gal A (agalsidase beta, Fabrazyme® or agalsidase alpha, Replagal®), but the clinical efficacy of this therapy is limited[5–7]. 1-Deoxygalactonojirimycin (Gal-DNJ **8**, Migalastat®, Figure 1B) has recently been approved as pharmacological chaperone (PC) for the treatment of Fabry disease in patients with amenable mutations[8]. Gal-DNJ **8** binds mutant forms of α-gal A, which are catalytically competent but otherwise targeted for degradation due to misfolding. Gal-DNJ **8** stabilizes the protein fold, allowing the mutant α-gal A to be trafficked to lysosomes. However, PC therapy for Fabry disease is limited to specific mutations and its efficacy is hotly debated[9–13]. For this reason, an attractive alternative therapeutic intervention strategy, proposed recently, comprises jointly-administering recombinant enzyme and a pharmacological chaperone[14–16]. This strategy aims to stabilize the recombinant enzyme in circulation such that larger proportions may reach disease affected tissues; permitting the use of extended intervals between injections and lower enzyme dosages which should diminish side effects, improve patient's life-style and reduce treatment costs[17,18]. For this strategy to become clinical practice, allosteric enzyme stabilizers or orthosteric competitive α-gal A inhibitors that prevent enzyme unfolding and are displaced by the accumulated metabolites in the lysosome recovering the glycosidase activity, with good selectivity and pharmacokinetic/ pharmacodynamic properties, are required[16,18,19]. We argue that the discovery of such commodities would be greatly facilitated by the design of new inhibitor templates.

Human α-gal A hydrolyzes its substrate following a Koshland double displacement mechanism, resulting in net retention of stereochemistry at the anomeric center of the produced galactopyranose[20,21]. The reaction coordinates by which α-gal A processes its substrate to form the intermediate covalent adduct are $^4C_1 \rightarrow {}^4H_3{}^{\ddagger} \rightarrow {}^1S_3$ with respect to the conformation of the galactopyranose moiety in the Michaelis complex → TS → covalent intermediate complex (Figure 1A)[22–24]. This same

[a] Department of Bio-organic Synthesis, Leiden Institute of Chemistry, Leiden University, Einsteinweg 55, 2333 CC Leiden, The Netherlands.
[b] Department of Medical Biochemistry, Leiden Institute of Chemistry. Einsteinweg 55, 2333 CC Leiden, The Netherlands.
[c] Department of Chemistry, York Structural Biology Laboratory, University of York, Heslington, York YO10 5DD, United Kingdom.
[d] Departament de Química Inorgànica i Orgànica (Secció de Química Orgànica) and Institut de Química Teòrica i Computacional (IQTCUB), Universitat de Barcelona, Martí i Franques 1, 08028 Barcelona, Spain.
[e] Fundació Catalana de Recerca i Estudis Avancats (ICREA), Passeig Lluís Companys 23, 08010 Barcelona, Spain.

*Corresponding authors. E-mail: h.s.overkleeft@lic.leidenuniv.nl; gideon.davies@york.ac.uk

† Electronic Supplementary Information (ESI) available: Supplementary Fig. S1 to S7, Table S1 and S2, materials and methods (biological and biochemical methods, DFT calculations, crystallography and chemical synthesis), and NMR spectra. See DOI: XXX.

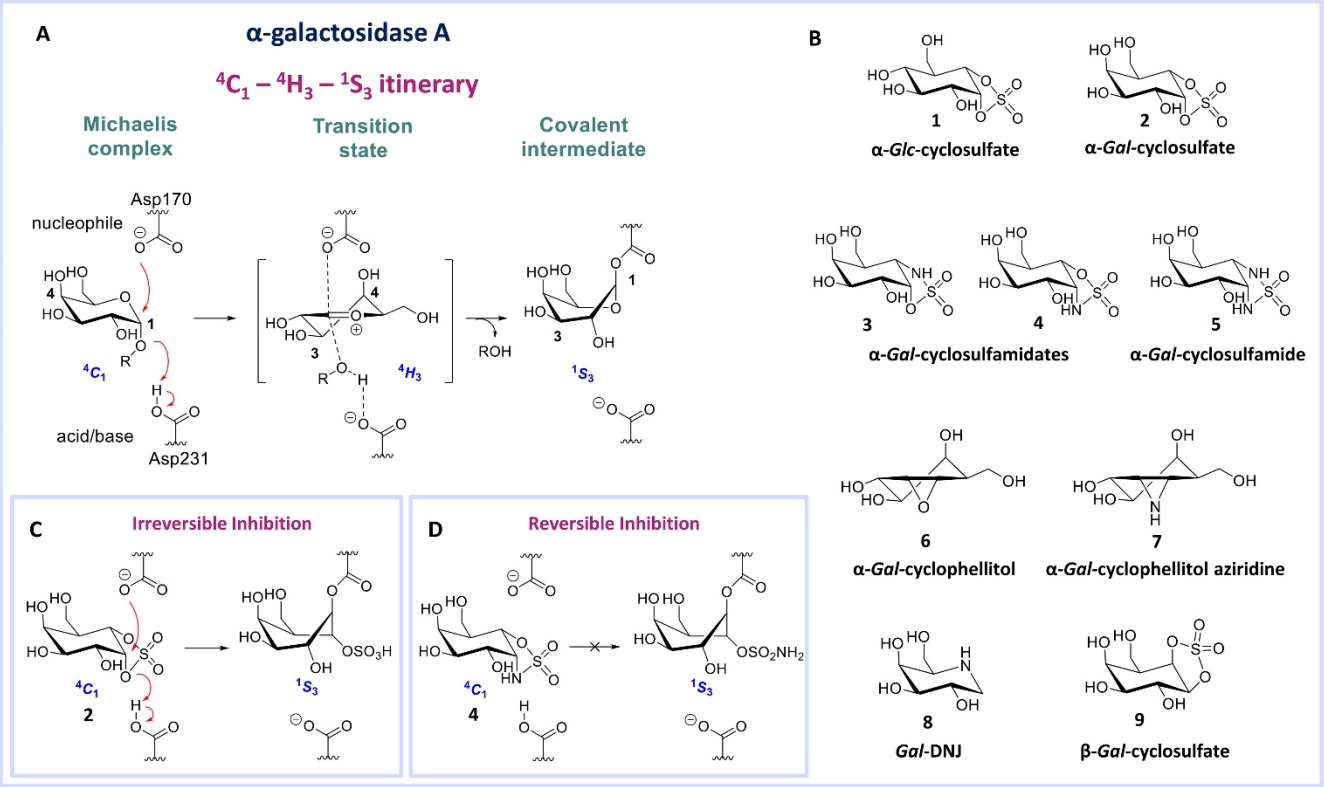

Figure 1. Reaction coordinates of α-galactosidases and inhibitors. A. Reaction itinerary of retaining α-galactosidase, showing conformations of the Michaelis complex, transition state, and covalent intermediate. B. Chemical structures of α-glucose configured cyclosulfate **1**, α-galactose configured cyclosulfate **2**, cyclosulfamidates **3** and **4**, cyclosulfamide **5**, cyclophellitol **6**, cyclophellitol aziridine **7**, 1-deoxygalactonojirimycin **8** and β-galactose configured cyclosulfate **9**. Galactose configured cyclosulfate **2** and cyclosulfamidate **4** inhibit α-galactosidases irreversibly (C) or reversibly (D) by mimicking the $^4C_1$ "Michaelis-like" conformation.

reaction itinerary is also employed by GH31 retaining α-glucosidases, with the difference that a glucopyranose, rather than a galactopyranose, is captured in the enzyme active site[25]. We have recently shown that α-*glc*-cyclosulfate **1** (Figure 1B) potently, selectively and irreversibly inhibits retaining α-glucosidases. Compound **1** in free solution predominantly resides in a $^4C_1$ chair conformation, thus mimicking the initial Michaelis complex conformation utilized by α-glucosidases[25] allowing facile interception by the catalytic nucleophile.

We reasoned that α-*gal*-cyclosulfate **2** would covalently and irreversibly inhibit α-gal A with equal efficiency and selectivity following the same mode of action (Figure 1B and 1C). Building on this concept, we further hypothesized that substitution of one or both of the cyclosulfate ring oxygens for nitrogen, as in compounds **3**-**5**, would lead to competitive α-gal A inhibitors because of the decreased leaving group capacity of cyclosulfamidates/cyclosulfamides, when compared to cyclosulfates (Figure 1D). Such compounds would then offer competitive enzyme inhibitors to be tested as stabilizers of recombinant α-galactosidase A for Fabry treatment. Here, we show the validity of this reasoning by revealing α-*gal*-cyclosulfamidate **4** as a first-in-class, effective and selective, competitive α-gal A inhibitor. Structural and computational analysis of the conformational behavior of compound **4** in solution and in the active site of human α-gal A supports our design and provides a molecular rationale why compound **4** is an effective α-gal A inhibitor. We also show compound **4** to be effective in stabilizing recombinant α-gal A *in vitro* and *in cellulo* and that sphingolipid levels in Fabry fibroblasts are effectively corrected by co-treatment with α-gal A and **4**.

Results

Synthesis of α-D-galactose configured cyclosulfate 2 and cyclosulfamidate 4.

Benzoylated diol **11** (see SI and Scheme S1 for its synthesis) was treated with thionyl chloride and subsequently oxidized with ruthenium trichloride and sodium periodate to afford protected cyclosulfate **12**. α-*Gal*-cyclosulfate **2** was obtained after benzoyl removal using methanolic ammonia (Scheme 1A). The synthesis of *cis*-1-amino-6-hydroxy cyclohexane **18**, a key intermediate in the synthesis of α-*gal*-cyclosulfamidate **4** proceeded through oxazolidinone **17**, which was obtained from *trans*-azido alcohol **13** (itself obtained from perbenzylated *galacto*-cyclophellitol, see the SI) as depicted in Scheme 1B. Hydrolysis of the carbamate in **17** and *N*-Bocylation provided **19**, which was transformed into fully protected cyclosulfamidate **20**. Global deprotection finally yielded the target compound **4**. The synthesis of compounds **3**, **5** and **9** (Figure 1B) and intermediates follows related strategies, as is described in the Supporting Information.

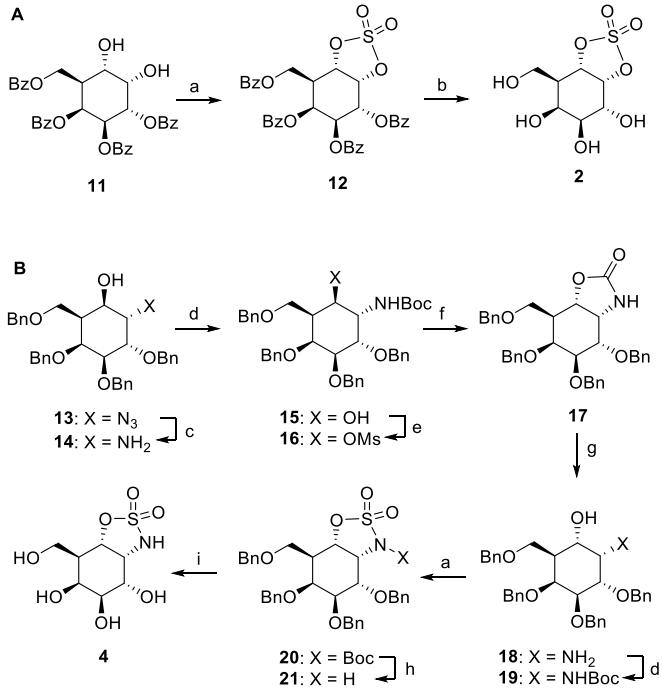

Scheme 1. Synthesis of α-D-galactose configured cyclosulfate **2** (A) and cyclosulfamidate **4** (B). Reagents and conditions: a) (i) $SOCl_2$, Et_3N, imidazole, DCM, 0 °C; (ii) $RuCl_3$, $NaIO_4$, CCl_4, MeCN, 0 °C, 3 h, **12**: 56 % and **20**: 59 %; b) NH_3, MeOH, rt, 3 h, 34 %; c) PtO_2, H_2, THF, rt, 4 h, 99 %; d) Boc_2O, Et_3N, DCM, rt, 16 h, **15**: 93% and **19**: 99 %; e) imidazole, MsCl, Et_3N, $CHCl_3$, rt, 16 h; f) DMF, 120 °C, 2 days, 47 % over 2 steps; g) 1 M NaOH, EtOH, 70 °C, 3 h, to rt, 16 h, 86 %; h) TFA, DCM, rt, 16 h, 71 %; i) $Pd(OH)_2$, H_2, MeOH, rt, 18 h, 57 %.

α-D-Galactose configured cyclosulfate 2, cyclosulfamidates 3 and 4, and cyclosulfamide 5 are predominantly in the $^4C_1$ conformation.

Free energy landscapes (FELs) of inhibitors report the conformational behavior in solution well, and can therefore be used to predict the selectivity for GH active sites[26]. We calculated conformational FELs of compounds **2**-**5** using *ab initio* metadynamics (Figure 2A, S1 and S2). The FEL of α-*gal*-cyclophellitol cyclosulfate **2** is strongly biased towards $^4C_1$, with a secondary minimum around $B_{2,5}$. This $B_{2,5}$ conformer is unlikely to be enzyme active-site-reactive as it exhibits an equatorial C1-O bond (Figure S2). The $^4C_1$ minimum of the substrate extends towards the TS-like $^4H_3$ conformation, indicating that cyclosulfate **2** in a $^4H_3$ conformation could be transiently populated on-enzyme, favoring the nucleophilic attack and formation of a glycosyl-enzyme adduct. The FELs of **3**-**5** show that substitution of the cyclic sulfate trap by cyclic sulfamidates (**3** and **4**) or sulfamide (**5**) does not significantly affect the conformational preferences. The local $B_{2,5}$ minimum in **4** is more pronounced, probably due to a hydrogen bond between the 2-OH and one cyclosulfamidate oxygen (Figure S2).

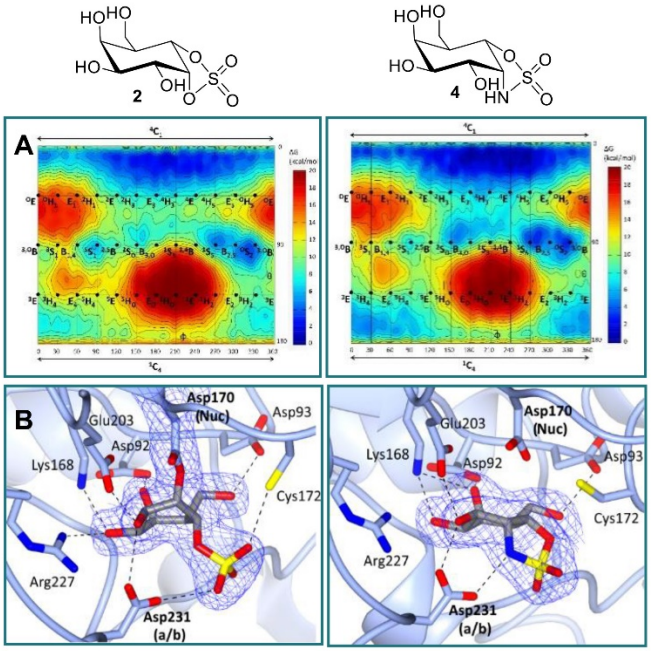

Figure 2. Conformational free energy landscapes and crystal structures of α-*gal*-cyclosulfate **2** and α-*gal*-cyclosulfamidate **4** in α-gal A (agalsidase beta). A. α-*Gal*-cyclosulfate **2** and α-*gal*-cyclosulfamidate **4** adopt $^4C_1$ ground state conformations. The x and y axes of each graph correspond to the ϕ and θ Cremer-Pople puckering coordinates (in degrees), respectively. Isolines are 1 kcal/mol. B. α-*Gal*-cyclosulfate **2** (left) reacts with the Asp170 nucleophile and adopts a $^1S_3$ conformation covalent adduct (i.e., "intermediate-like") in complex with agalsidase beta. Unreacted **4** (right) in complex with agalsidase beta adopts a $^4C_1$ "Michaelis-like" conformation in the active site. Electron density for protein side chains and ligands is REFMAC maximum-likelihood/σA-weighted $2F_o - F_c$ contoured to 0.21 electrons/Å^3 for **2** and **4**. nuc = nucleophile; a/b = acid/base.

α-D-Galactose configured cyclosulfate 2 and isosteres 4 and 5 inhibit α-gal A *in vitro*.

α-*Gal*-cyclosulfate **2**, α-*gal*-cyclosulfamidates **3** and **4**, α-*gal*-cyclosulfamide **5**, as well as the known α-galactosidase inhibitors α-*gal*-cyclophellitol **6**[27], α-*gal*-cyclophellitol aziridine **7**[27], *Gal*-DNJ **8**[28] and β-*gal*-cyclosulfate **9** were evaluated on their inhibitory potential against recombinant human GH27 α-galactosidase A (α-gal A, Fabrazyme®, agalsidase beta) and their selectivity over human β-galactosidases, galactosidase beta 1 (GLB1, GH35) and galactosylceramidase (GALC, GH59). We first determined apparent IC_{50} values by using fluorogenic 4-methylumbelliferyl (4MU)-α- or -β-D-galactopyranose substrates (Table 1). α-*Gal*-cyclosulfate **2** effectively inhibits α-gal A on a par with α-*gal*-cyclophellitol **6** (apparent IC_{50} = 25 *vs* 13 µM, respectively), although less potently than α-*gal*-cyclophellitol aziridine **7** (apparent IC_{50} = 40 nM). Cyclosulfamidate **4**, with the sulfamidate nitrogen taking up the position occupied by the anomeric oxygen in the natural substrate, proved to be a rather good inhibitor (IC_{50} = 67 µM), whereas isomer **3** is inactive and sulfamide **5** considerably less potent (IC_{50} = 423 µM).

Table 1. Apparent IC_{50} values for *in vitro* inhibition of human recombinant α-galactosidase A (agalsidase beta), β-galactosidase GLB1 in human fibroblast lysates and GALC overexpressed in HEK293 cells. Inactivation rates and inhibition constants (k_{inact} and K_I) in human recombinant α-galactosidase A (agalsidase beta); N.D., not determined; [a]due to weak inhibition; [b]due to fast inhibition; N.A., not applicable. Reported values are mean ± standard deviation from 3 technical replicates.

Compd.	*In vitro* α-gal A (agalsidase beta) apparent IC_{50} (μM)	*In vitro* β-gal (GLB1) apparent IC_{50} (μM)	*In vitro* β-gal (GALC) apparent IC_{50} (μM)	Kinetic Parameters α-gal A (agalsidase beta) k_{inact} (min^{-1}) and K_I (μM) or K_i (μM)	Kinetic Parameters α-gal A (agalsidase beta) k_{inact}/K_I ($min^{-1}\mu M^{-1}$)
α-*Gal*-cyclosulfate 2	25 ± 2.5	>1000	>1000	Irreversible K_I = 237 kinact = 0.06	0.25
α-*Gal*-cyclosulfamidate 3	>1000	39 ± 4.6	95 ± 14	N.A.	N.A.
α-*Gal*-cyclosulfamidate 4	67 ± 4.7	>1000	>1000	Competitive K_i = 110	-
α-*Gal*-cyclosulfamide 5	423 ± 58	38 ± 1.7	191 ± 5.5	N.D.[a]	N.D.[a]
α-*Gal*-cyclophellitol 6	13 ± 0.95	0.84 ± 0.13	4.2 ± 0.51	Irreversible K_I = 430 k_{inact} = 0.24	0.55
α-*Gal*-cyclophellitol azidiridine 7	0.040 ± 0.005	0.93 ± 0.06	1.1 ± 0.30	Irreversible N.D.[b]	16.4
Gal-DNJ 8	0.079 ± 0.004	42 ± 0.72	433 ± 39	Competitive K_i = 0.23	-
β-*Gal*-cyclosulfate 9	>1000	>1000	>1000	N.A.	N.A.

We also measured the apparent IC_{50} values for inhibition against two human β-galactosidases: GLB1 (measured in human fibroblast lysates) and GALC (measured in overexpressing HEK293 cell medium). Cyclosulfate **2** and cyclosulfamidate **4** appear to be more selective than cyclophellitol epoxide **6** and aziridine **7**, and we reason this to be due to the $^4C_1$ conformation adopted by **2** and **4**, which corresponds to the Michaelis complex conformation in α-galactosidases, but not in β-galactosidases (compound **2** is inactive up to 1 mM whereas **6** and **7** display low micromolar activity towards GLB1 and GALC). β-*Gal*-cyclosulfate **9**, which in principle neither mimics the Michaelis complex nor the transition state conformation of β-galactosidases[29,30], is inactive against β- and α-galactosidases up to 1 mM. Cyclosulfamidate **4** and Gal-DNJ **8** show selectivity over α-glucosidase GAA, whereas both inhibit human recombinant β-glucosidase (GBA) (Table S1).

We next explored the reversibility of inhibition by our new cyclic sulfate analogues. Enzymes were pre-incubated for different time periods (30, 60, 120, 240 min) with inhibitors at concentrations of their corresponding apparent IC_{50} values, after which residual α-gal A activity was determined (Figure S3). Whilst cyclosulfate **2** is an irreversible inhibitor (a decrease in α-galactosidase activity with longer incubation time), cyclosulfamidate **4** and cyclosulfamide **5** were reversible inhibitors as revealed by a constant residual activity with extended incubation times. This was confirmed by kinetic studies monitoring the absorbance generated by the hydrolysis of 2,4-dinitrophenyl-α-D-galactopyranoside substrate (2,4-DNP-α-gal) (Table 1). The irreversible inhibitors **2**, **6** and **7** follow pseudo-first order kinetics. Although α-cyclosulfate **2** has a similar k_{inact}/K_I ratio as α-cyclophellitol **6** (k_{inact}/K_I = 0.25 vs 0.55 $min^{-1}mM^{-1}$, respectively), it has a stronger initial binding constant (K_I) and a slower inactivation rate constant (k_{inact}) (**2**: K_I = 237 μM and k_{inact} = 0.06 min^{-1}; **6**: K_I = 430 μM and k_{inact} = 0.24 min^{-1}). Only a k_{inact}/K_I ratio could be measured for α-aziridine **7** due to fast inhibition (k_{inact}/K_I = 16.4 $min^{-1}mM^{-1}$). Kinetics with increasing 2,4-DNP-α-gal concentrations showed that cyclosulfamidate **4** reversibly inhibits α-galactosidase with a K_i of 110 μM.

Structural analysis of α-*gal*-cyclosulfate 2 and α-*gal*-cyclosulfamidate 4 in complex with agalsidase beta.

Firstly, in order to confirm the covalent inhibition by the cyclic sulfate, the X-ray structure of agalsidase beta in complex with **2** (PDB:6IBM) was determined to 1.99 Å, revealing a single molecule of **2** covalently bound to the enzyme active site (Figure 2B). The observed electron density unambiguously shows that α-cyclosulfate **2** has reacted by attack of the catalytic nucleophile, Asp 170, to form a covalent enzyme-inhibitor complex. This covalent complex adopts a $^1S_3$ conformation, consistent with the conformation of the covalent intermediate in the α-galactosidase reaction itinerary (Figure 1A). Upon nucleophilic attack to the cyclic sulfate, the sulfate forms hydrogen bonds with Asp231 and Cys172, the latter suffering a shift in position.

Armed with the knowledge that **2** indeed forms a covalent adduct to agalsidase beta, we moved onto ascertain if the cyclosulfamidate **4** would, as envisaged, function as a non-

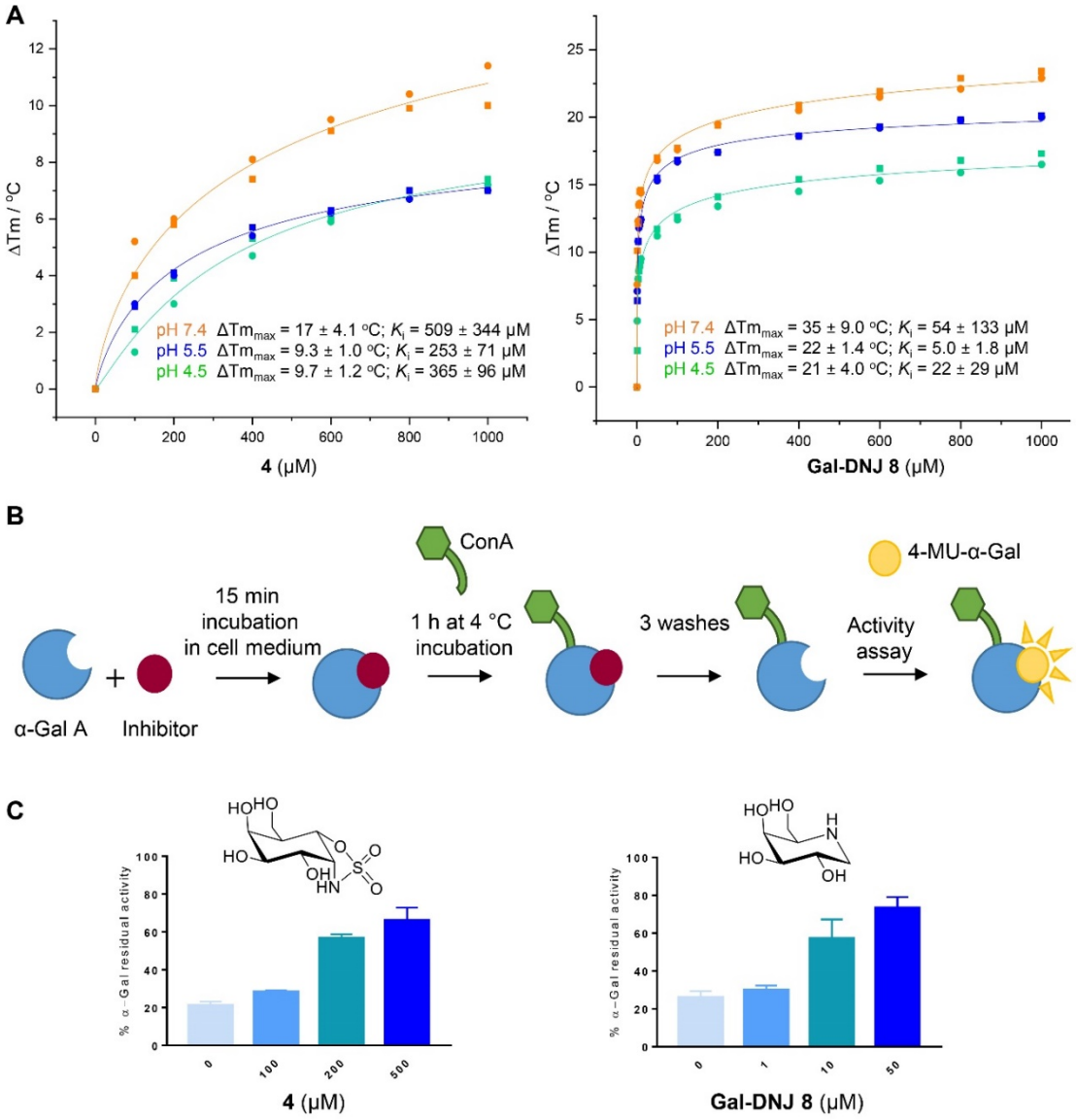

Figure 3. Effect of α-cyclosulfamidate **4** and Gal-DNJ **8** on thermal stability and cell culture medium stability of agalsidase. A. Heat-induced melting profiles of lysosomal α-gal A recorded by thermal shift, measured at pH 4.5, 5.5 and 7.4 in the presence of α-cyclosulfamidate **4** and Gal-DNJ **8**. Melting points (Tm) were determined through thermal shift analyses by monitoring the florescence of Sypro Orange dye (λ_{em} 585 nm) as a function of temperature (see supplementary information). B. Schematic representation of stabilization effect assay. Agalsidase beta was incubated with inhibitor for 15 min in DMEM/F-12 medium and subsequently incubated with ConA sepharose beads for 1 h at 4 °C and washed to remove inhibitor. Residual α-Gal activity was quantified with 4-MU-α-gal substrate. C. Percentage of α-gal A residual activity after 15 min incubation in DMEM/F-12 medium in the presence of inhibitor α-g*al*-cyclosulfamidate **4** (at 0, 100, 200, 500 μM) and Gal-DNJ **8** (0, 1, 10 and 50 μM), followed by post final ConA purification. Percentages are calculated considering the 100 % activity of α-gal A obtained at 0 min incubation time (n=2, error bars indicate mean ± standard deviation).

covalent, active-centre-directed, inhibitor of the enzyme-replacement enzyme. In contrast to cyclosulfate **2**, cyclosulfamidate **4** (PDB: 6IBK determined to 2.07 Å) was indeed shown to reversibly bind the catalytic site (Figure 2B). As expected, the α-galactose configured cyclosulfamidate **4** adopts a $^4C_1$ "Michaelis-like" complex conformation in the active site. Interestingly, the NH from the cyclosulfamidate moiety forms a hydrogen bond with the acid/base Asp231.

Thermostability of agalsidase beta in the presence of α-cyclosulfamidate 4 and Gal-DNJ 8.

Competitive α-galactosidase inhibitors, including Gal-DNJ **8,** are currently investigated in clinical studies as stabilizers of recombinant enzyme, where they are deployed to enhance enzyme replacement efficacy. In such a treatment regime, enzyme and active site inhibitor are administered jointly[11,14,16]. The stability of a recombinant enzyme relative to the temperature is considered to reflect well its stability in body circulation[31], and can be measured with ease, also in the presence of competitive inhibitors designed to stabilize protein fold[31,32]. Accordingly, we performed thermal stability assays (TSAs) on agalsidase beta alone and in the presence of increasing concentrations of **2**, **4** or **8**.

Thermal melting profiles of lysosomal α-gal A revealed that α-gal A is most thermostable at pH 5.5 (Figure 3A and S4), which

is consistent with α-gal A being a lysosomal enzyme. α-*Gal*-cyclosulfamidate **4** stabilizes α-gal A at pH 7.4 with a ΔTm_{max} of 17.4 °C, compared to a ΔTm_{max} of 34.3 °C produced by Gal-DNJ **8** (Figure 3A and S4). TSA effects at acidic pHs were lower for both **4** and Gal-DNJ **8**, with recorded ΔTm_{max} values of 9.3 °C and 22.3 °C for **4** and Gal-DNJ **8**, respectively at pH 5.5, and ΔTm_{max} values of 9.7 °C and 21.2 °C for the same compounds at pH 4.5. Surprisingly, we observed no thermostabilization effect on α-gal A in the presence of α-*gal*-cyclosulfate **2**, despite this compound being an irreversible α-galactosidase inhibitor. Possibly, the sulfate group does not provide the optimal enzyme-ligand interactions to induce stabilization of α-galactosidase when the ring is in $^1S_3$ conformation adopted by covalently bound **2**, compared to the $^4C_1$ conformations adopted by both **4** and Gal-DNJ **8**.

Stabilization of agalsidase beta by α-cyclosulfamidate 4 in cell culture medium.

Agalsidase beta shows poor stability in plasma at pH of 7.3 - 7.4, with only ~25 % of the hydrolytic activity being retained after incubation of enzyme at 1 µg/mL in human plasma for 30 minutes[33]. Given the stabilizing effect observed for **4** in the above described TSAs, we investigated the ability of this compound to stabilize agalsidase beta in culture medium at physiological pH compared to Gal-DNJ **8**[34].We first investigated the stabilization effect of the inhibitors in culture medium alone, as surrogate measure for plasma stability (Figure 3B and 3C). Incubation of agalsidase beta (25 µL of 2.5 µg/µL) in cell culture medium (Dulbecco's Modified Eagles Medium/Nutrient Mixture F-12 (DMEM/F12), supplemented with 10 % fetal calf serum and 1 % penicillin/streptomycin) led to 80 % loss of activity within 15 min, in line with the poor stability of this enzyme in blood plasma. To assess the stabilizing effects of **2**, **4** and Gal-DNJ **8** in cell culture media, agalsidase beta was incubated with increasing concentrations of these compounds, followed by capture of the enzyme on concanavalin A (ConA) sepharose beads, washing to remove bound inhibitor, and quantification of residual α-galactosidase activity with 4MU-α-gal substrate. Media stabilization of agalsidase beta followed the same trend as observed in TSAs, with **2** failing to stabilize the enzyme and instead irreversibly inhibiting agalsidase beta. In contrast, α-*gal*-cyclosulfamidate **4** and Gal-DNJ **8** both prevented inactivation of agalsidase beta in cell culture media (pH 7.2) - ~75 % residual α-*gal*-A activity was retained after incubation with **4** (at 500 µM) or Gal-DNJ **8** (at 50 µM) (Figure 3C).

Competitive activity-based protein profile (ABPP) on recombinant α-galactosidases.

We studied the binding of α-cyclosulfamidate **4** and Gal-DNJ **8** to the commercial α-galactosidases: agalsidase beta (Fabrazyme®), agalsidase alpha (Replagal®) and α-galactosidase B (*N*-acetylgalactosaminidase, NAGA) by competitive activity-based protein profiling (ABPP, Figure 4). Enzymes were incubated with increasing concentrations (ranging from 0 to 1000 µM) of both α-cyclosulfamidate **4** and Gal-DNJ **8** for 30 min at 37 °C, followed by incubation with 0.2 µM of an α-galactosidase Cy5 activity-based probe (ABP **10**, Figure S5) for 30 min at 37 °C. After incubation the samples were analyzed by

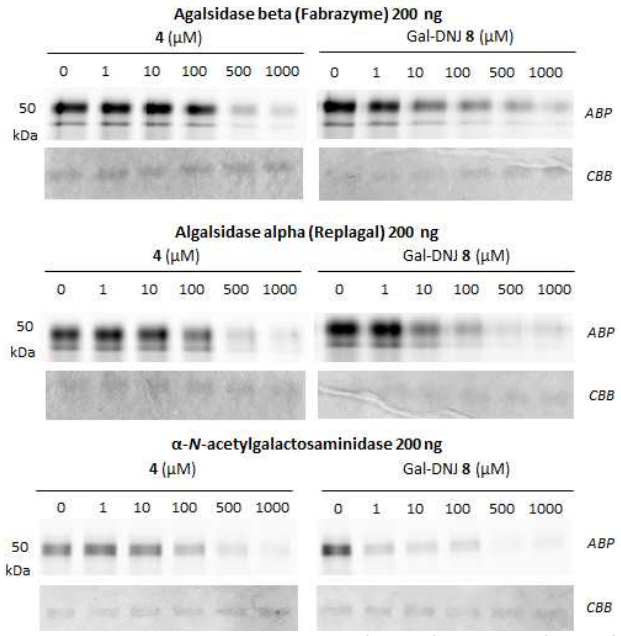

Figure 4. Competitive ABPP in α-galactosidases. α-Galactosidases (agalsidase beta 200 ng and agalsidase alpha 200 ng) and α-*N*-acetylgalactosaminidase (NAGA, 200 ng) were pre-incubated with α-cyclosulfamidate **4** (0-1000 µM) or Gal-DNJ **8** (0-1000 µM) for 30 min followed by fluorescent labelling with Cy5 α-galactosidase ABP **10**. ABP: activity-based probe, CBB: coomassie brilliant blue staining.

sodium dodecyl sulfate-polyacrylamide gels (SDS- PAGE), followed by fluorescent scan of the gels as previously described[27,33]. Competitive ABPP revealed that α-cyclosulfamidate **4** (100-500 µM) and Gal-DNJ **8** (1-10 µM) inhibit both recombinant human α-galactosidases and *N*-acetylgalactosaminidase.

***In situ* treatment of cultured fibroblasts from patients with Fabry disease.**

We next investigated whether the stabilizing effect of α-cyclosulfamidate **4** towards agalsidase beta produced an improvement in the cellular uptake of the enzyme by fibroblasts. We performed *in situ* studies in 5 different primary cell lines obtained from adult male volunteers: wild-type (WT, Control) representing normal α-gal A activity, 2 classic Fabry mutant fibroblasts (R301X and D136Y) with no α-gal A activity and 2 atypical variant Fabry mutants (A143T and R112H) with substantially lowered residual α-gal A activity. Fibroblasts were incubated with 0.5 % DMSO (untreated) or either **4** (200 µM) or Gal-DNJ **8** (20 µM) (in blue), agalsidase beta (100 ng) or with a combination of both enzyme and stabilizing agent (in green) (Figure 5A). After 24 h treatment, the cells were harvested and homogenized, and the intracellular α-gal A activity of the corresponding cell lysates was measured. WT cell line presented normal α-gal A activity whereas untreated classic Fabry patients (R301X and D136Y) and variant mutation samples (A143T and R112H) showed reduced enzymatic activity. None of the cell lines, not even classical Fabry fibroblasts R301X and D136Y, showed significant increase in α-gal A activity when incubated with **4** (200 µM) or **8** (20 µM) alone for 24 h. Of note, Gal-DNJ **8** is known to enhance α-gal A activity in R301Q lymphoblasts after *in situ* 4-day treatment of a 100 µM daily dose.[34] Treatment with agalsidase beta showed a considerable increase in α-gal A activity in all the studied cell lines. This effect was improved in

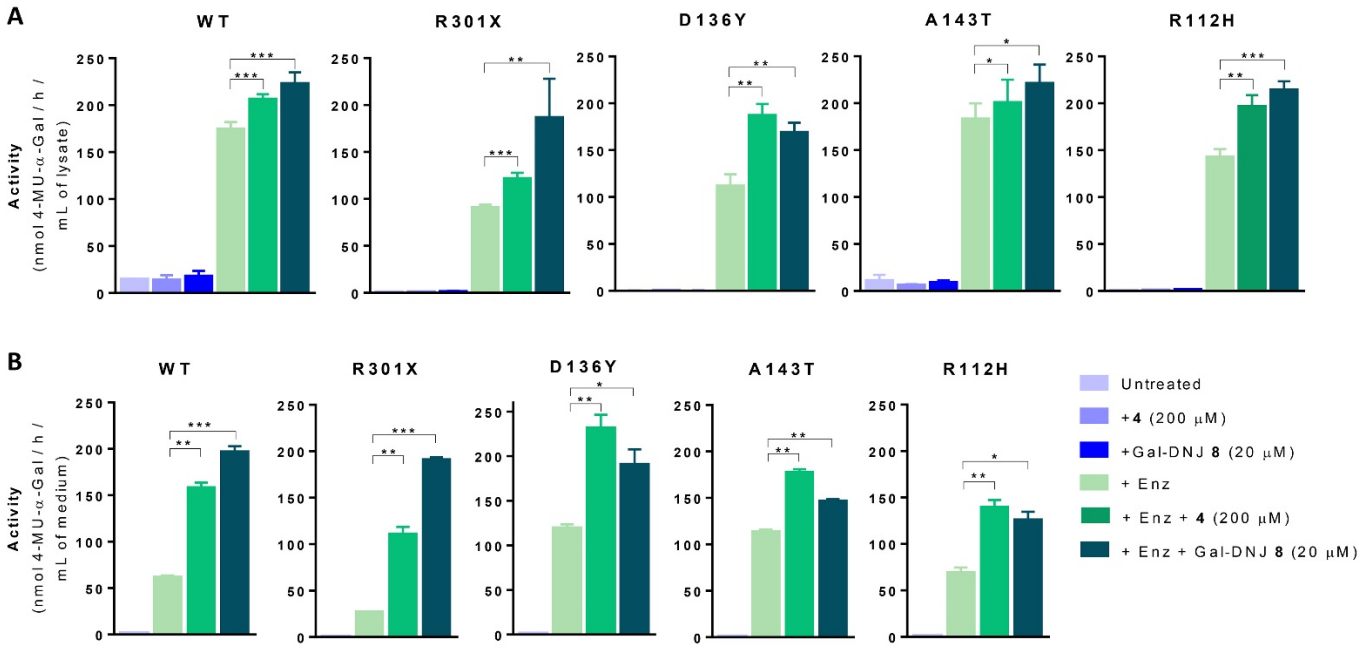

Figure 5. Effect on α-gal A activity in fibroblasts culture and medium following treatment with α-cyclosulfamidate **4** and Gal-DNJ **8**. A. Fibroblasts of WT, classic Fabry (R301X and D136Y) and variant Fabry (A143T and R112H) were untreated or incubated with α-cyclosulfamidate **4** (200 μM), Gal-DNJ **8** (20 μM), agalsidase beta (200 ng/mL) or a combination of enzyme and stabilizing agent for 24 h. Then, the medium was collected, cells were harvested, and α-gal A activity was measured in the cell homogenates by 4-MU-α-gal assay. In all cell lines co-administration of α-cyclosulfamidate **4** or Gal-DNJ **8** with agalsidase beta increased intracellular α-gal A activity when compared to cells treated with only agalsidase beta. B. α-Gal A activity in cell culture medium samples was measured after ConA purification. α-Gal A activity is at least two times higher in all the cell lines treated with α-cyclosulfamidate **4** (200 μM) or Gal-DNJ **8** (20 μM). Reported activities are mean ± standard deviation from two biological replicates, each with two technical replicates, * $p < 0.5$; **, $p < 0.01$; ***, $p < 0.001$.

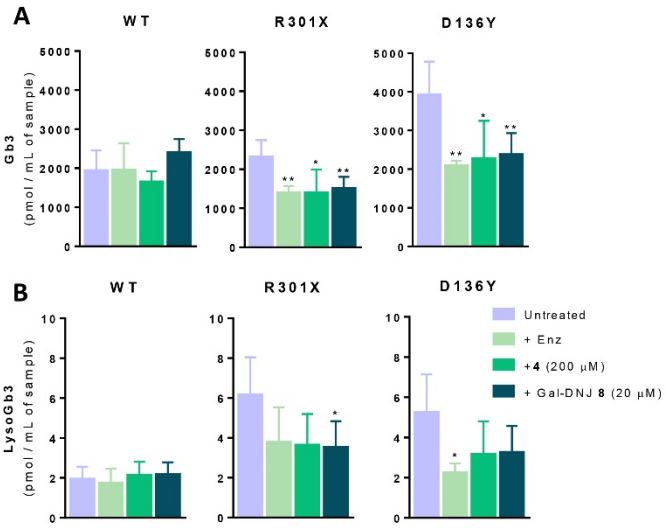

Figure 6. Gb3 and Lyso-Gb3 quantification in cultured fibroblasts treated with agalsidase beta co-administrated with α-cyclosulfamidate **4** and Gal-DNJ **8**. Gb3 (A) and lysoGb3 (B) levels (pmol/mL of sample) measured by LC-MS/MS in Fabry fibroblasts from WT and classic Fabry patients (R301X and D136Y) treated with agalsidase beta (200 ng/mL) with or without α-cyclosulfamidate **4** (200 μM) and Gal-DNJ **8** (20 μM) for 24 h. Reported activities are mean ± standard deviation from two biological replicates, each with two technical replicates, * $p < 0.5$; **, $p < 0.01$

most cases with the combinatorial treatment of agalsidase beta and **4** or **8** after 24 h incubation. We also measured α-gal A activity in media in order to confirm that the increase in α-gal A activity in cell lysates is due to stabilization of the enzyme (Figure 5B). Thus, culture media were collected before harvesting the cells and α-gal A activity was measured after ConA purification. α-Gal A activity in media was at least double in all the cell lines treated with α-cyclosulfamidate **4** (200 μM) or Gal-DNJ **8** (20 μM), consisting with these compounds preventing α-gal A degradation during cell culture.

Gb3 and LysoGb3 levels are corrected by α-cyclosulfamidate 4.

Generally, Fabry patients present elevated Gb3 which is further metabolized by acid ceramidase into LysoGb3 in lysosomes[35]. LysoGb3 constitutes a signature of Fabry disease and allows diagnostic monitoring of disease progression[2,3,36–38], and has been linked to neuronopathic pain and renal failure through its effect on nociceptive neurons and podocytes[39–42]. We investigated whether co-administration of α-cyclosulfamidate **4** and Gal-DNJ **8** with agalsidase beta would also have a positive effect in correcting these toxic metabolite levels. Gb3 and lysoGb3 levels from *in situ* treated cells were measured by LC-MS/MS (Figure 6). Normal Gb3 and lysoGb3 levels observed in wild-type cells range around 2000 pmol/mL and 2 pmol/mL of Gb3 and lysoGb3, respectively. Cultured fibroblasts from classic Fabry patients (R301X and D136Y) treated with agalsidase beta resulted in a reduction of Gb3 and lysoGb3. This reduction was similar when fibroblasts were treated with the combination of α-cyclosulfamidate **4** (200 μM) or Gal-DNJ **8** (20 μM) and agalsidase beta. Variant Fabry A143T cell line presents normal Gb3 and lysoGb3 basal levels, whereas in R112H fibroblasts, these metabolites are increased and not corrected by agalsidase beta itself or inhibitor-agalsidase beta combination treatment (Figure S6).

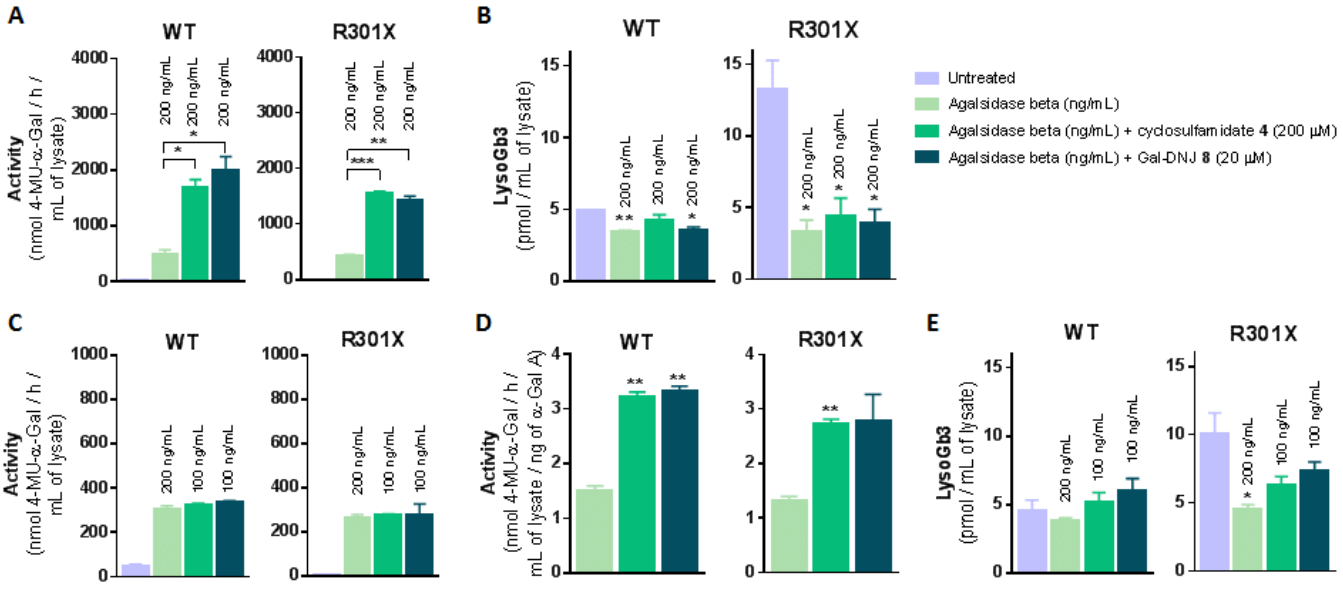

Figure 7. Effect on α-gal A activity and Lyso-Gb3 correction in cultured fibroblasts treated with α-cyclosulfamidate **4** and Gal-DNJ **8.** Fibroblasts of WT and classic Fabry (R301X) were incubated with agalsidase beta (200 ng/mL) or the combination of enzyme (200 ng/mL or 100 ng/mL) and stabilizing agent (**4** 200 μM or **8** 20 μM) for 4 days. Then, the medium was collected, cells were harvested, and α-gal A activity was measured in the cell homogenates by 4-MU-α-gal assay. **A**. Intracellular α-gal A activity in fibroblasts treated with agalsidase beta (200 ng/mL) or the combination of α-cyclosulfamidate **4** (200 μM) or Gal-DNJ **8** (20 μM) with agalsidase beta (200 ng/mL) for 4 days. **B**. LysoGb3 levels measured by LC-MS/MS in Fabry fibroblasts from panel A. **C**. Intracellular α-gal A activity is comparable in cell lines treated with the combination of α-cyclosulfamidate **4** (200 μM) or Gal-DNJ **8** (20 μM) but this requires only half the concentration of agalsidase beta (100 ng/mL). **D**. Intracellular α-gal A activity per ng of agalsidase beta in fibroblasts treated with agalsidase beta (100 ng/mL) or the combination of α-cyclosulfamidate **4** (200 μM) or Gal-DNJ **8** (20 μM) with half concentration of agalsidase beta (100 ng/mL). **E**. LysoGb3 levels measured by LC-MS/MS in Fabry fibroblasts from panel C or D. Reported lipid levels are mean ± standard deviation from two biological replicates, each with two technical replicates, * $p < 0.5$; **, $p < 0.01$; ***, $p < 0.001$.

***In situ* 4-day treatment of cultured fibroblasts: increased α-gal A activity and Gb3 metabolites correction by α-cyclosulfamidate 4.**

We next investigated whether the beneficial effect could be potentiated by extended incubation treatments. Thus, WT and classic Fabry (R301X) fibroblasts were treated with agalsidase beta (200 ng/mL) or with a combination of enzyme (200 ng/mL) and α-cyclosulfamidate **4** (200 μM) or Gal-DNJ **8** (20 μM) for 4 days. Fibroblasts were treated every 24 h with new medium and/or enzyme with or without inhibitor, and medium samples were collected for α-gal A activity quantification (See supporting information, Figure S7). α-Gal A activity was 3-4 times higher in fibroblasts treated with the combination of recombinant α-gal A and α-cyclosulfamidate **4** (200 μM) or Gal-DNJ **8** (20 μM) than those treated with agalsidase beta alone (Figure 7A). This increase in α-gal A activity correlates with the reduction of Lyso-Gb3 from ~14 pmol/mL to ~4 pmol/mL in the cell lysates of Fabry (classic R301X) fibroblasts (Figure 7B). We finally studied whether the amount of required ERT could be decreased when stabilized with **4** or Gal-DNJ **8** and still produce a similar effect. WT and Fabry (classic R301X) fibroblasts were treated with agalsidase beta at 200 ng/mL and 100 ng/mL. A reduction in toxic metabolites can be achieved in 4 days with half the concentration of enzyme (100 ng/mL) when either α-cyclosulfamidate **4** (200 μM) or Gal-DNJ (20 μM) is added (Figure 7C,D), with a similar reduction of toxic Lyso-Gb3 from ~10 pmol/mL to ~5-6 pmol/mL in the cell lysates of Fabry (classic R301X) fibroblasts (Figure 7E).

Discussion

ERT with intravenous administration of recombinant human α-D-galactosidase (agalsidase beta, Fabrazyme® or agalsidase alpha, Replagal®) reduces the levels of Gb3 and lyso-Gb3 in some tissues of Fabry patients, but its clinical efficacy is still limited[5–7,43]. The limited enzyme stability in plasma is a major drawback, and it is for this reason that enzyme active site binders that stabilize recombinant enzyme in circulation are pursued – with Gal-DNJ **8** (Migalastat®) currently in use in the clinic as the benchmark. Here we report the design and synthesis of the first-in-class conformational glycosidase inhibitor and α-gal A stabilizing agent, α-cyclosulfamidate **4**. We show that this compound reversibly and selectively inhibits agalsidase beta with an IC_{50} value of 67 μM and a K_i of 110 μM. *Ab initio* metadynamics calculations and structural analysis of α-cyclosulfamidate **4** in complex with agalsidase beta show that this inhibitor binds in a $^4C_1$ conformation mimicking the Michaelis complex conformation. We demonstrate that α-cyclosulfamidate **4** stabilizes recombinant human α-D-galactosidase (agalsidase beta, Fabrazyme®) in thermal stabilization assays and show that this prevents its degradation in cell culture medium. We further show that both α-*gal*-cyclosulfamidate **4** and Gal-DNJ **8** stabilize the enzyme more significantly at neutral pH than under acidic conditions (ΔTm_{max} difference of 8.1 °C for **4** and ΔTm_{max} difference of 12.2 °C for Gal-DNJ **8**).

To further study the stabilizing effect, we investigated whether α-*gal*-cyclosulfamidate **4** and Gal-DNJ **8** would stabilize α-gal A activity *in situ* cell conditions. Treatment of fibroblasts (WT, classic and variant Fabry cell lines) with only α-*gal*-cyclosulfamidate **4** (at 200

μM) and Gal-DNJ **8** (at 20 μM) for 24 h shows no effect on α-D-galactosidase activity. However, we observe an increased α-D-galactosidase activity in all cells treated with the combination of agalsidase beta and stabilizing agents (**4** at 200 μM and **8** at 20 μM) when compared to the cells treated only with agalsidase beta. This result also correlates with an increased α-D-galactosidase activity in the cell medium of the cells treated with enzyme and **4** or **8**. The stabilizing effect is more pronounced when cells are treated for longer time (4 days), suggesting that the agalsidase beta complexed with α-*gal*-cyclosulfamidate **4** or Gal-DNJ **8** is stabilized in the cell medium, internalized and dissociated from the reversible inhibitor in the lysosomes. Finally, co-administration of α-cyclosulfamidate **4** or Gal-DNJ **8** with agalsidase beta highlights a similar correction of toxic Gb3 and lyso-Gb3 metabolite levels as with the ERT alone. Importantly, similar α-gal A activity and correction of toxic metabolites is achieved with half the concentration of agalsidase beta when this is stabilized by α-cyclosulfamidate **4** or Gal-DNJ **8**. The synergy between Gal-DNJ **8** and the human recombinant α-gal A in cultured fibroblasts from Fabry patients has recently been demonstrated both in agalsidase alpha and beta[16,19]. This synergism, together with our agalsidase beta stabilization results, supports the idea that the efficacy of a combination treatment may be superior to ERT or PC alone for several reasons. Co-administration of ERT and active site inhibitor may be effective in all Fabry patients, independent of mutations in their endogenous α-gal A. Furthermore, stabilization of the recombinant human α-gal A by a stabilizing agent may reduce the required enzyme dosages or extend IV injections intervals, and therefore improve patient's life-style and reduce side effects and treatment costs.

Conclusions

In conclusion, we have developed a new class of α-D-galactosidase inhibitors based on cyclophellitol cyclosulfamidate as a conformational Michaelis complex isostere. Although cyclosulfamidate **4** is a 1000-fold weaker inhibitor of recombinant α-gal A compared to Gal-DNJ **8** *in vitro*, it stabilizes α-gal A *in cellulo* at only 10 fold higher concentration, and we argue that non-basic, competitive glycosidase inhibitors are attractive starting points for clinical development as stabilizers of (recombinant) glycosidases in the context of lysosomal storage disorders. As well, compound **4** and its structural isosteres (**3** and **5**) comprise a new class of competitive glycosidase inhibitors that stabilize agalsidase beta for the first time, not by the glycoside configurational mimicry and basic nature that is the hallmark of iminosugars (including Migalastat®), but by configurational and conformational mimicry of the Michaelis complex. Michaelis complex or product-like conformational competitive inhibitors have been reported that act on other glycosidases, for instance, thio-oligosacharides[44–46] and kifunensine[47,48]. We believe that transferring the structural characteristics of our cyclosulfamidates to differently configured structural analogues may yield potent and selective competitive inhibitors targeting other glycosidases and that these may have biological or biomedical value in their own right, be it as stabilizing agents or as classical enzyme inhibitors.

Conflicts of interest

There are no conflicts to declare.

Author contributions

M.A., J.M.F.G.A., H.S.O. and G.J.D. conceived and designed the experiments. M.A., C.H. and A.S. carried out synthesis of inhibitors under supervision of G.A.v.d.M and J.D.C.C. L.R. performed *Ab Initio* metadynamic calculations under supervision of C.R. R.R. and L.W. carried out structural studies on enzyme-inhibitor complexes and thermostability assays under supervision of G.J.D. M.A., M.J.G. and K.K. determined IC_{50} values and kinetic parameters, performed agalsidase beta stabilization studies *in vitro* and *in cellulo*, and lipid metabolites quantification. M.A., J.M.F.G.A., G.J.D and H.S.O. wrote the manuscript with input from all authors.

Acknowledgements

We thank The Netherlands Organization for Scientific Research (NWO-CW, ChemThem grant to J.M.F.G.A. and H.S.O., and NOW TOP grant 2018-714.018.002 to H.S.O.), the European Research Council (ERC-2011-AdG- 290836 "Chembiosphing", to H.S.O., and ERC-2012-AdG- 322942 "Glycopoise", to G.J.D.), Sanofi Genzyme (research grant to J.M.F.G.A. and H.S.O. for financial support and postdoctoral contract to M.A.), the Spanish Ministry of Science, Innovation and Universities (MICINN) and the European Regional Development Fund (FEDER) (CTQ2017-85496-P to C. R.), the Agency for Management of University and Research Grants of *Generalitat de Catalunya* (AGAUR) (2017SGR-1189 to C. R.) and the Spanish Structures of Excellence María de Maeztu (MDM-2017-0767 to C.R.). R.J.R. is supported by the BBSRC (BB/M011151/1). We thank the Diamond Light Source for access to beamline i02 and i04 (proposal number mx-13587) and the computer resources at *MareNostrum* and the technical support provided by Barcelona Supercomputing Center (proposal RES-QCM-2017-2-0011). G.J.D. is supported by the Royal Society though the Ken Murray Research Professorship.

References

1 V. Lombard, H. Golaconda Ramulu, E. Drula, P. M. Coutinho and B. Henrissat, *Nucleic Acids Res.*, 2014, **42**, 490–495.

2 J. M. Aerts, J. E. Groener, S. Kuiper, W. E. Donker-Koopman, A. Strijland, R. Ottenhoff, C. van Roomen, M. Mirzaian, F. A. Wijburg, G. E. Linthorst, A. C. Vedder, S. M. Rombach, J. Cox-Brinkman, P. Somerharju, R. G. Boot, C. E. Hollak, R. O. Brady and B. J. Poorthuis, *Proc. Natl. Acad. Sci.*, 2008, **105**, 2812–2817.

3 H. Gold, M. Mirzaian, N. Dekker, M. J. Ferraz, J. Lugtenburg, J. D. C. Codée, G. A. Van Der Marel, H. S. Overkleeft, G. E. Linthorst, J. E. M. Groener, J. M. Aerts and B. J. H. M. Poorthuis, *Clin. Chem.*, 2013, **59**, 547–556.

4 R. J. Desnick, Y. a. Ioannou and C. M. Eng, *OMMBID Online Metab. Mol. Bases Inherit. Dis.*, , DOI:10.1036/ommbid.181.

5 M. Arends, M. Biegstraaten, D. A. Hughes, A. Mehta, P. M. Elliott, D. Oder, O. T. Watkinson, F. M. Vaz, A. B. P. Van Kuilenburg, C. Wanner and C. E. M. Hollak, *PLoS One*, 2017, **12**, 1–17.

6 M. Arends, F. A. Wijburg, C. Wanner, F. M. Vaz, A. B. P. van Kuilenburg, D. A. Hughes, M. Biegstraaten, A. Mehta, C. E. M. Hollak and M. Langeveld, *Mol. Genet. Metab.*, 2017, **121**, 157–161.

7 T. Alegra, F. Vairo, M. V de Souza, B. C. Krug and I. V. D.

Schwartz, *Genet. Mol. Biol.*, 2012, **35**, 947–954.
8 A. Markham, *Drugs*, 2016, **76**, 1147–1152.
9 F. E. Mohamed, L. Al-Gazali, F. Al-Jasmi and B. R. Ali, *Front. Pharmacol.*, 2017, **8**, 448.
10 S. Ishii, H.-H. Chang, K. Kawasaki, K. Yasuda, H.-L. Wu, S. C. Garman and J.-Q. Fan, *Biochem. J.*, 2007, **406**, 285–295.
11 E. R. Benjamin, J. J. Flanagan, A. Schilling, H. H. Chang, L. Agarwal, E. Katz, X. Wu, C. Pine, B. Wustman, R. J. Desnick, D. J. Lockhart and K. J. Valenzano, *J. Inherit. Metab. Dis.*, 2009, **32**, 424–440.
12 D. A. Hughes, K. Nicholls, S. P. Shankar, G. Sunder-Plassmann, D. Koeller, K. Nedd, G. Vockley, T. Hamazaki, R. Lachmann, T. Ohashi, I. Olivotto, N. Sakai, P. Deegan, D. Dimmock, F. Eyskens, D. P. Germain, O. Goker-Alpan, E. Hachulla, A. Jovanovic, C. M. Lourenco, I. Narita, M. Thomas, W. R. Wilcox, D. G. Bichet, R. Schiffmann, E. Ludington, C. Viereck, J. Kirk, J. Yu, F. Johnson, P. Boudes, E. R. Benjamin, D. J. Lockhart, C. Barlow, N. Skuban, J. P. Castelli, J. Barth and U. Feldt-Rasmussen, *J. Med. Genet.*, 2017, **54**, 288–296.
13 G. Sunder-Plassmann, R. Schiffmann and K. Nicholls, *Expert Opin. Orphan Drugs*, 2018, **6**, 301–309.
14 C. Porto, M. Cardone, F. Fontana, B. Rossi, M. R. Tuzzi, A. Tarallo, M. V. Barone, G. Andria and G. Parenti, *Mol. Ther.*, 2009, **17**, 964–971.
15 E. R. Benjamin, R. Khanna, A. Schilling, J. J. Flanagan, L. J. Pellegrino, N. Brignol, Y. Lun, D. Guillen, B. E. Ranes, M. Frascella, R. Soska, J. Feng, L. Dungan, B. Young, D. J. Lockhart and K. J. Valenzano, *Mol. Ther.*, 2012, **20**, 717–726.
16 C. Porto, A. Pisani, M. Rosa, E. Acampora, V. Avolio, M. R. Tuzzi, B. Visciano, C. Gagliardo, S. Materazzi, G. La Marca, G. Andria and G. Parenti, *J. Inherit. Metab. Dis.*, 2012, **35**, 513–520.
17 D. G. Warnock, D. G. Bichet, M. Holida, O. Goker-Alpan, K. Nicholls, M. Thomas, F. Eyskens, S. Shankar, M. Adera, S. Sitaraman, R. Khanna, J. J. Flanagan, B. A. Wustman, J. Barth, C. Barlow, K. J. Valenzano, D. J. Lockhart, P. Boudes and F. K. Johnson, *PLoS One*, 2015, **10**, 1–17.
18 J. Castelli, S. Sitaraman, D. J. Lockhart, K. Nicholls, P. F. Boudes, R. Giugliani, D. P. Germain, D. A. Hughes, C. J. Jennette, A. Mehta, A. Bragat and L. Barisoni, *Orphanet J. Rare Dis.*, 2012, **7**, 91.
19 A. Pisani, C. Porto, G. Andria and G. Parenti, *J. Inherit. Metab. Dis.*, 2014, **37**, 145–146.
20 H. Brumer, P. F. G. Sims and M. L. Sinnott, *Biochem. J.*, 1999, **339**, 43–53.
21 A. I. Guce, N. E. Clark, E. N. Salgado, D. R. Ivanen, A. A. Kulminskaya, H. Brumer and S. C. Garman, *J. Biol. Chem.*, 2010, **285**, 3625–3632.
22 D. E. Koshland, *Biol. Rev.*, 1953, **28**, 416–436.
23 D. L. Zechel and S. G. Withers, *Acc. Chem. Res.*, 2000, **33**, 11–18.
24 G. Speciale, A. J. Thompson, G. J. Davies and S. J. Williams, *Curr. Opin. Struct. Biol.*, 2014, **28**, 1–13.
25 M. Artola, L. Wu, M. J. Ferraz, C. L. Kuo, L. Raich, I. Z. Breen, W. A. Offen, J. D. C. Codée, G. A. Van Der Marel, C. Rovira, J. M. F. G. Aerts, G. J. Davies and H. S. Overkleeft, *ACS Cent. Sci.*, 2017, **3**, 784–793.
26 R. J. Williams, J. Iglesias-Fernández, J. Stepper, A. Jackson, A. J. Thompson, E. C. Lowe, J. M. White, H. J. Gilbert, C. Rovira, G. J. Davies and S. J. Williams, *Angew. Chemie - Int. Ed.*, 2014, **53**, 1087–1091.
27 L. I. Willems, T. J. M. Beenakker, B. Murray, S. Scheij, W. W. Kallemeijn, R. G. Boot, M. Verhoek, W. E. Donker-Koopman, M. J. Ferraz, E. R. Van Rijssel, B. I. Florea, J. D. C. Codée, G. A. Van Der Marel, J. M. F. G. Aerts and H. S. Overkleeft, *J. Am. Chem. Soc.*, 2014, **136**, 11622–11625.
28 G. Legler and S. Pohl, *Carbohydr. Res.*, 1986, **155**, 119–129.
29 N. F. Bráa, P. A. Fernandes and M. J. Ramos, *J. Chem. Theory Comput.*, 2010, **6**, 421–433.
30 R. W. Wheatley, S. Lo, L. J. Jancewicz, M. L. Dugdale and R. E. Huber, *J. Biol. Chem.*, 2013, **288**, 12993–13005.
31 R. L. Lieberman, J. A. D'Aquino, D. Ringe and G. A. Petsko, *Biochemistry*, 2009, **48**, 4816–4827.
32 J. Q. Fan, S. Ishii, N. Asano and Y. Suzuki, *Nat. Med.*, 1999, **5**, 112–115.
33 K. Kytidou, T. J. M. Beenakker, L. B. Westerhof, C. H. Hokke, G. F. Moolenaar, N. Goosen, M. Mirzaian, M. J. Ferraz, M. de Geus, W. W. Kallemeijn, H. S. Overkleeft, R. G. Boot, A. Schots, D. Bosch and J. M. F. G. Aerts, *Front. Plant Sci.*, 2017, **8**, 1026.
34 N. Asano, S. Ishii, H. Kizu, K. Ikeda, K. Yasuda, A. Kato, O. R. Martin and J. Q. Fan, *Eur. J. Biochem.*, 2000, **267**, 4179–4186.
35 M. J. Ferraz, A. R. A. Marques, M. D. Appelman, M. Verhoek, A. Strijland, M. Mirzaian, S. Scheij, C. M. Ouairy, D. Lahav, P. Wisse, H. S. Overkleeft, R. G. Boot and J. M. Aerts, *FEBS Lett.*, 2016, **590**, 716–725.
36 H. Maruyama, K. Miyata, M. Mikame, A. Taguchi, C. Guili, M. Shimura, K. Murayama, T. Inoue, S. Yamamoto, K. Sugimura, K. Tamita, T. Kawasaki, J. Kajihara, A. Onishi, H. Sugiyama, T. Sakai, I. Murata, T. Oda, S. Toyoda, K. Hanawa, T. Fujimura, S. Ura, M. Matsumura, H. Takano, S. Yamashita, G. Matsukura, R. Tazawa, T. Shiga, M. Ebato, H. Satoh and S. Ishii, *Genet. Med.*, 2019, **21**, 44–52.
37 M. Mirzaian, P. Wisse, M. J. Ferraz, A. R. A. Marques, P. Gaspar, S. V. Oussoren, K. Kytidou, J. D. C. Codée, G. van der Marel, H. S. Overkleeft and J. M. Aerts, *Clin. Chim. Acta*, 2017, **466**, 178–184.
38 M. Mirzaian, P. Wisse, M. J. Ferraz, A. R. A. Marques, T. L. Gabriel, C. P. A. A. van Roomen, R. Ottenhoff, M. van Eijk, J. D. C. Codée, G. A. van der Marel, H. S. Overkleeft and J. M. Aerts, *Clin. Chim. Acta*, 2016, **459**, 36–44.
39 L. Choi, J. Vernon, O. Kopach, M. S. Minett, K. Mills, P. T. Clayton, T. Meert and J. N. Wood, *Neurosci. Lett.*, 2015, **594**, 163–168.
40 M. D. Sanchez-Niño, D. Carpio, A. B. Sanz, M. Ruiz-Ortega, S. Mezzano and A. Ortiz, *Hum. Mol. Genet.*, 2015, **24**, 5720–5732.
41 P. Colpart and S. Félix, *Arch. Pathol. Lab. Med.*, 2017, **141**, 1127–1131.
42 P. Rozenfeld and S. Feriozzi, *Mol. Genet. Metab.*, 2017, **122**, 19–27.
43 L. van Dussen, M. Biegstraaten, C. E. M. Hollak and M. G. W. Dijkgraaf, *Orphanet J. Rare Dis.*, 2014, **9**, 1–12.
44 G. Sulzenbacher, H. Driguez, B. Henrissat, M. Schülein and G. J. Davies, *Biochemistry*, 1996, **35**, 15280–15287.
45 A. J. Thompson, J. Dabin, J. Iglesias-Fernández, A. Ardèvol, Z. Dinev, S. J. Williams, O. Bande, A. Siriwardena, C. Moreland, T. C. Hu, D. K. Smith, H. J. Gilbert, C. Rovira and G. J. Davies, *Angew. Chemie - Int. Ed.*, 2012, **51**, 10997–11001.
46 Y. Zhu, M. D. L. Suits, A. J. Thompson, S. Chavan, Z. Dinev,

C. Dumon, N. Smith, K. W. Moremen, Y. Xiang, A. Siriwardena, S. J. Williams, H. J. Gilbert and G. J. Davies, *Nat. Chem. Biol.*, 2010, **6**, 125–132.

47 F. Vallée, K. Karaveg, A. Herscovics, K. W. Moremen and P. L. Howell, *J. Biol. Chem.*, 2000, **275**, 41287–41298.

48 A. Males, L. Raich, S. J. Williams, C. Rovira and G. J. Davies, *ChemBioChem*, 2017, **18**, 1496–1501.